

# Usefulness of diffusion-weighted MR imaging for differentiating between Warthin's tumor and oncocytoma of the parotid gland

Hiroki Kato<sup>1</sup> · Keita Fujimoto<sup>1</sup> · Masayuki Matsuo<sup>1</sup> · Keisuke Mizuta<sup>2</sup> · Mitsuhiro Aoki<sup>2</sup>

Received: 14 November 2016 / Accepted: 27 December 2016 / Published online: 10 January 2017  
© Japan Radiological Society 2017

## Abstract

**Purpose** To assess the efficacy of diffusion-weighted (DW) MR imaging for differentiating between Warthin's tumor and oncocytoma of the parotid gland.

**Methods** Forty-five histopathologically confirmed parotid gland tumors (41 Warthin's tumors and 4 oncocytomas) were examined by MR imaging including DW imaging. <sup>18</sup>F-fluorodeoxyglucose PET/CT was also performed in 9 Warthin's tumors and 3 oncocytomas. We retrospectively reviewed the images and compared the MR signal intensities, apparent diffusion coefficients (ADCs), and maximum standardized uptake values (SUVmax) of the solid components between the two pathologies.

**Results** The signal intensity ratios (SIRs) on both T2-weighted images ( $0.92 \pm 0.18$  vs  $0.65 \pm 0.13$ ,  $p < 0.01$ ) and DW images ( $1.24 \pm 0.42$  vs  $0.43 \pm 0.16$ ,  $p < 0.001$ ) were higher in Warthin's tumors than in oncocytomas. ADCs ( $0.79 \pm 0.11$  vs  $1.06 \pm 0.06 \times 10^{-3} \text{ mm}^2/\text{s}$ ,  $p < 0.001$ ) were lower in Warthin's tumors than in oncocytomas. No significant differences in the SIRs on T1-weighted images ( $1.09 \pm 0.12$  vs  $0.99 \pm 0.07$ ,  $p = 0.051$ ) and SUVmax ( $8.22 \pm 3.86$  vs  $8.11 \pm 1.33$ ,  $p = 0.864$ ) were found between Warthin's tumor and oncocytoma.

**Conclusion** DW imaging with ADC measurements is useful for the differentiation of Warthin's tumor from oncocytoma of the parotid gland.

**Keywords** Diffusion-weighted imaging · Parotid gland · Warthin's tumor · Oncocytoma

## Introduction

Warthin's tumor, also known as adenolymphoma, cystadenolymphoma, or papillary cystadenoma lymphomatosum, is the second most common tumor of the salivary glands. It primarily affects male patients during the sixth and seventh decades of life. Its etiology is unknown, but there is a strong association with cigarette smoking. It is almost exclusively restricted to the parotid gland and the periparotid lymph node. The great majority of these tumors are located in the lower pole of the parotid gland. It presents multifocally in 21–38% of cases and bilaterally in 6–29% of cases [1, 2].

Oncocytoma, also known as oncocyticadenoma or oxyphilicadenoma, is a rare benign epithelial tumor accounting for about 1% of all salivary gland neoplasms. It usually presents in elderly patients in the sixth to eighth decades of life, and there is no gender predilection. It occurs most commonly in the parotid gland and the remaining arises in the submandibular gland. About 20% of patients with oncocytoma have a history of radiation exposure 5 or more years before tumor discovery. The incidence of bilateral oncocytoma is about 7% [3], often distributed in both the superficial and deep lobes.

In evaluating neoplasms of the salivary gland, it is well known that the accumulation of <sup>99m</sup>Tc-perchnetate is almost pathognomonic of Warthin's tumor and oncocytoma. Although many previous articles have reported MR imaging findings, including diffusion-weighted (DW) imaging of Warthin's tumor [4–6] and oncocytoma [7–9], we failed to find any reports comparing MR imaging

✉ Hiroki Kato  
hkato@gifu-u.ac.jp

<sup>1</sup> Department of Radiology, Gifu University School of Medicine, 1-1 Yanagido, Gifu 501-1194, Japan

<sup>2</sup> Department of Otolaryngology, Gifu University School of Medicine, Gifu, Japan

**Table 1** Patient characteristics

Characteristics	Warthin's tumor	Oncocytoma
Number of patients	41	4
Age (year)		
Range	45–83	49–78
Mean	63.8	64.3
Gender		
Male	36	0
Female	5	4
Reference standard		
Tumorectomy	30	4
Biopsy	11	0

findings of Warthin's tumor and oncocytoma. Therefore, the purpose of this study was to evaluate the differences in MR imaging findings including DW imaging between Warthin's tumor and oncocytoma.

## Materials and methods

### Patients

The present study was approved by the human research committee of the institutional review board of our hospital, and complied with the guidelines of the Health Insurance Portability and Accountability Act of 1996. The requirement for informed consent was waived due to the retrospective nature of this study. We searched the electronic medical records at our university hospital for patients with histopathologically proven Warthin's tumor or oncocytoma of the parotid gland who had undergone preoperative MR imaging, including DW imaging between June 2006 and August 2016. We found 48 patients with Warthin's tumor and 4 patients with oncocytoma. However, 7 patients with purely cystic Warthin's tumor were excluded from this study.

In total, 41 patients with Warthin's tumor (age range, 45–83 years; mean age, 63.8 years; 36 men and 5 women) and 4 patients with oncocytoma (age range, 49–78 years; mean age, 64.3 years; 4 women) were included in this study. Although 10 patients with Warthin's tumor had multifocal or bilateral tumors, only MR images of the largest tumors were assessed. All patients with oncocytoma had a solitary tumor. Thus, 41 Warthin's tumors and 4 oncocytomas were evaluated in this study. The histopathological diagnosis of 30 Warthin's tumors and 4 oncocytomas was established by surgical excision, and 11 Warthin's tumors were diagnosed by biopsy. Patients' characteristics are summarized in Table 1.

### MR imaging

A 1.5-T MR imaging system (Intera Achieva 1.5 T Pulsar, Philips Medical Systems, Best, the Netherlands) was used. Transverse MR images were obtained using the parallel imaging technique at 4-mm section thickness with 1-mm intersection gap. Non-fat suppressed T1-weighted spin-echo (TR/TE, 620–827/9–15 ms; imaging matrices, 512 × 512; field of view, 20 × 20 cm, parallel imaging factor, 1.5) and non-fat suppressed T2-weighted fast spin-echo (TR/TE, 4102–5710/90 ms; imaging matrices, 512 × 512; field of view, 20 × 20 cm, parallel imaging factor, 1.5), and DW short-tau inversion recovery (STIR) single-shot spin-echo echo-planar (TR/TE/TI, 5490/72/170 ms; imaging matrices, 256 × 256; field of view, 40 × 40 cm; b-value, 0 and 1000 s/mm<sup>2</sup>; parallel imaging factor, 1.8) images were obtained.

### <sup>18</sup>F-fluorodeoxyglucose (FDG) PET/CT

Whole-body PET/CT (Biograph Sensation 16; Siemens Medical Solutions, Malvern, PA, USA) from the skull to mid-thigh was performed for 9 patients with Warthin's tumor and 3 patients with oncocytoma. Briefly, after at least 4 h of fasting, patients received an intravenous injection of <sup>18</sup>F-FDG (185 MBq). Blood glucose levels were checked in all patients before FDG injection, and no patient had a blood glucose level greater than 150 mg/dl. Approximately 60 min after FDG injection, CT and subsequent whole-body PET were performed.

Technical parameters of the 16-row multidetector CT were; a gantry rotation speed of 0.5 s, a table speed of 24 mm per gantry rotation, and quiet-breathing data acquisition. Transverse images were reconstructed with 2-mm section thickness and no overlap. Oral or intravenous contrast agent was not used for CT. PET had an axial view of 16.2 cm per bed position with an intersectional gap of 3.75 mm in one bed position, which necessitated data acquisition in six or seven bed positions. Axial PET images were obtained using an imaging matrix of 256 × 256 and a field of view of 50 × 50 cm.

### Image assessment

A radiologist with 17 years of post-training experience in head and neck imaging reviewed all MR images. The reviewer was unaware of patient names, laboratory results, other imaging findings, or final diagnoses.

For the quantitative measurements, the reviewer measured the maximum and minimum diameters of the parotid gland tumors. If the parotid gland tumors were multifocal or bilateral, only the largest parotid gland tumor was assessed. Subsequently, the reviewer defined the regions

**Table 2** Quantitative measurements of Warthin's tumor and oncocytoma

	Warthin's tumor ( <i>n</i> = 41)	Oncocytoma ( <i>n</i> = 4)	<i>p</i> value
Maximum diameter (mm)	22.4 ± 8.5	14.8 ± 6.0	0.069
Minimum diameter (mm)	16.2 ± 6.5	10.5 ± 4.4	0.075
Tumor-to-spinal cord signal intensity ratios			
T2-weighted images	0.92 ± 0.18	0.65 ± 0.13	0.006*
T1-weighted images	1.09 ± 0.12	0.99 ± 0.07	0.051
Diffusion-weighted images	1.24 ± 0.42	0.43 ± 0.16	0.000*
ADC values ( $\times 10^{-3}$ mm <sup>2</sup> /s)	0.79 ± 0.11	1.06 ± 0.06	0.000**
SUVmax	8.22 ± 3.86	8.11 ± 1.33	0.864

Data are shown as the mean ±1 standard deviation

\* The value of Warthin's tumors was significant higher than those of oncocytomas ( $p < 0.01$ )

\*\* The value of Warthin's tumors was significant lower than those of oncocytomas ( $p < 0.01$ )

of interest (ROIs) and recorded the MR signal intensities. ROIs were placed as broadly as possible in the solid components of the tumors while excluding cystic components. The reviewer also measured signal intensities of the spinal cord at the same level as the tumors and calculated the tumor-to-spinal cord signal intensity ratios (SIRs). Apparent diffusion coefficient (ADC) values [ $\times 10^{-3}$  mm<sup>2</sup>/s] were measured on ADC maps by placing ROIs over the tumors. ROIs were placed to encompass lesions as much as possible while avoiding cystic components by referring to the T2-weighted images. For the semi-quantitative analysis of FDG uptake, the reviewer determined the maximum standardized uptake value (SUVmax) of each lesion.

For the qualitative assessments, the reviewer evaluated the number (solitary or multiple) and laterality (hemilateral or bilateral) of the parotid gland tumors. In the largest parotid gland tumors, the location (upper/mid pole or lower pole) of the parotid glands and the presence of intratumoral cystic components were also assessed.

### Statistical analysis

All statistical analyses were performed using SPSS version 22.0 (SPSS, Inc, an IBM Company, Chicago, Illinois, USA). The Mann–Whitney *U* test was used to compare the size, MR signal intensities, ADCs, and SUVmax between Warthin's tumors and oncocytomas. The chi-square test and Fisher's exact test were performed to compare the frequency of the multiplicity, bilaterality, location, and intratumoral cysts of the tumors between the two pathologies. Null hypotheses of no difference were rejected if *p*-values were less than 0.05.

### Results

The quantitative measurements are summarized in Table 2 and Fig. 1. No significant differences were found between

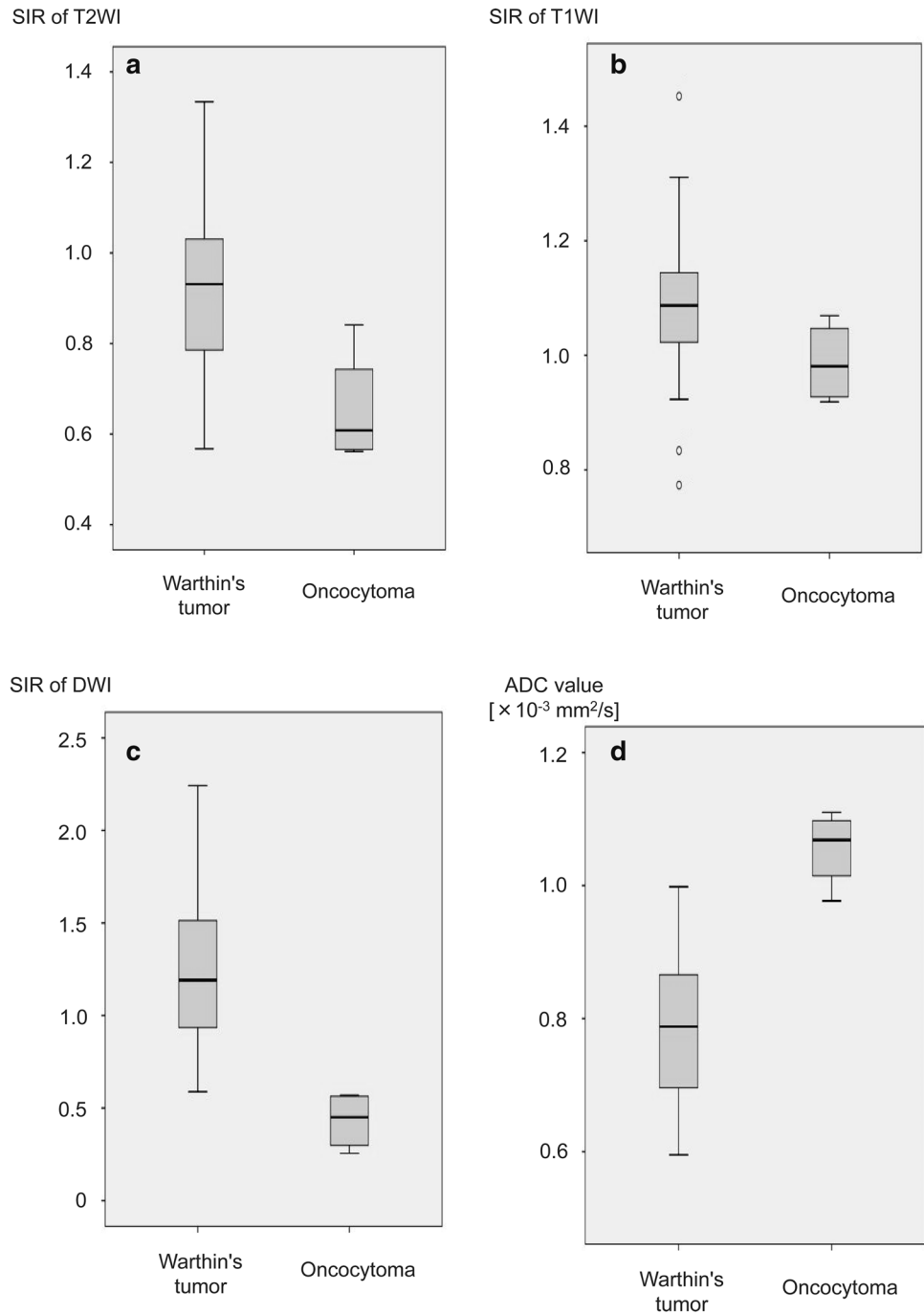
Warthin's tumors and oncocytomas regarding the maximum tumor diameter (22.4 ± 8.5 vs 14.8 ± 6.0 mm,  $p = 0.069$ ), minimum tumor diameter (16.2 ± 6.5 vs 10.5 ± 4.4 mm,  $p = 0.075$ ), and ratios of maximum to minimum diameters (1.41 ± 0.23 vs 1.42 ± 0.12,  $p = 0.577$ ). The SIRs on T2-weighted images (0.92 ± 0.18 vs 0.65 ± 0.13,  $p < 0.01$ ) and those on DW images (1.24 ± 0.42 vs 0.43 ± 0.16,  $p < 0.001$ ) were higher in Warthin's tumors than in oncocytomas (Figs. 2, 3). ADCs (0.79 ± 0.11 vs 1.06 ± 0.06  $\times 10^{-3}$  mm<sup>2</sup>/s,  $p < 0.001$ ) were lower in Warthin's tumors than in oncocytomas (Figs. 2, 3). No significant differences were found between Warthin's tumors and oncocytomas regarding the SIRs on T1-weighted images (1.09 ± 0.12 vs 0.99 ± 0.07,  $p = 0.051$ ) and SUVmax (8.22 ± 3.86 vs 8.11 ± 1.33,  $p = 0.864$ ).

The qualitative imaging findings are summarized in Table 3. The location of lower pole (88 vs 25%,  $p < 0.05$ ) was more frequent in Warthin's tumors than in oncocytomas. No significant differences were found between Warthin's tumors and oncocytomas regarding the frequency of multiplicity (24 vs 0%,  $p = 0.351$ ), bilaterality (12 vs 0%,  $p = 0.613$ ), and intratumoral cysts (37 vs 0%,  $p = 0.184$ ).

### Discussion

In the imaging for autoimmune and inflammatory disease of the salivary gland, <sup>99m</sup>Tc-pertechnetate scintigraphy may be useful for assessing salivary gland function. In evaluating salivary gland neoplasms, the accumulation of <sup>99m</sup>Tc-pertechnetate is almost pathognomonic of Warthin's tumor and oncocytoma. Because <sup>99m</sup>Tc-pertechnetate retention within Warthin's tumor is well differentiated from the normal parotid gland, which drains <sup>99m</sup>Tc-pertechnetate after gustatory stimulation, <sup>99m</sup>Tc-pertechnetate scintigraphy with gustatory stimulation is useful for the detection and differentiation of Warthin's

**Fig. 1** Box and whisker plots showing quantitative measurements of SIRs on T2-weighted, T1-weighted, and DW images, and ADCs of the two pathologies. Boundary of *boxes* closest to zero indicates 25th percentile, *line within boxes* indicates median, and *boundary of boxes* farthest from zero indicates 75th percentile. *Error bars* indicate smallest and largest values within 1.5 box lengths of 25th and 75th percentiles. *Outliers* are represented as individual points. **a** SIRs on T2-weighted images were higher in Warthin's tumors ( $0.92 \pm 0.18$ ) than in oncocytomas ( $0.65 \pm 0.13$ ) ( $p < 0.01$ ). **b** No significant differences were found between Warthin's tumors ( $1.09 \pm 0.12$ ) and oncocytomas ( $0.99 \pm 0.07$ ) regarding the SIRs on T1-weighted images ( $p = 0.051$ ). **c** SIRs on DW images were higher in Warthin's tumors ( $1.24 \pm 0.42$ ) than in oncocytomas ( $0.43 \pm 0.16$ ) ( $p < 0.001$ ). **d** ADCs were lower in Warthin's tumors ( $0.79 \pm 0.11 \times 10^{-3} \text{ mm}^2/\text{s}$ ) than in oncocytomas ( $1.06 \pm 0.06 \times 10^{-3} \text{ mm}^2/\text{s}$ ) ( $p < 0.001$ )



tumor [10, 11]. Reports suggest that the degree of uptake in Warthin's tumor on  $^{99\text{m}}\text{Tc}$ -pertechnetate scintigraphy after gustatory stimulation depends on the tumor size [2, 12], histologic subtype [12], and presence of large cystic components [2]. The increased concentrations of  $^{99\text{m}}\text{Tc}$ -pertechnetate have also been observed in oncocytomas [13]. Warthin's tumor and oncocytoma concentrate pertechnetate because they originate from the salivary duct epithelium [14].

Pleomorphic adenomas are the most common parotid gland tumors, and their characteristic MR imaging findings have been previously reported. On T2-weighted images, pleomorphic adenoma is typically demonstrated as a hyperintense lesion with lobulated contours. On DW imaging, ADCs of pleomorphic adenomas were significantly higher than those of all other entities, except for myoepithelial adenomas [6]. In addition, pleomorphic adenoma does not retain  $^{99\text{m}}\text{Tc}$ -pertechnetate, in contrast to Warthin's tumor

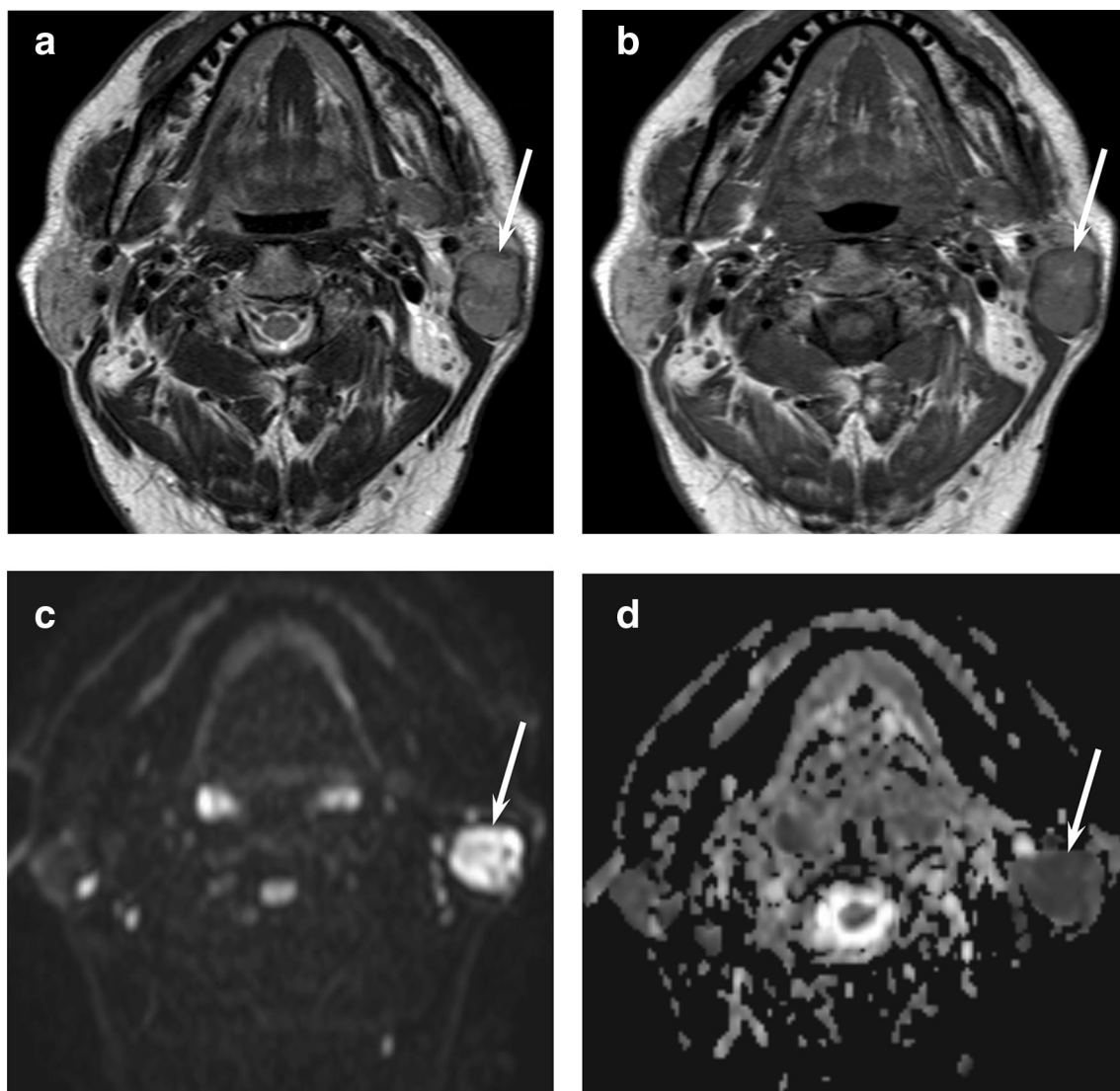


**Fig. 2** A 59-year-old man with Warthin's tumors of the parotid gland. **a** T2-weighted MR image (TR/TE, 4102/90 ms) shows a homogeneously isointense lesion (*arrow*) in lower pole of the left parotid gland. **b** T1-weighted MR image (TR/TE, 779/15 ms)

shows an isointense lesion (*arrow*). **c** DW MR image (TR/TE/TI, 5490/72/170 ms) shows a strong hyperintense lesion (*arrow*). **d** ADC map shows low ADC value ( $0.69 \times 10^{-3} \text{ mm}^2/\text{s}$ ) (*arrow*)

and oncocytoma. Therefore, MR imaging or  $^{99\text{m}}\text{Tc}$ -pertechnetate scintigraphy can usually differentiate pleomorphic adenoma from Warthin's tumor and oncocytoma. However,  $^{99\text{m}}\text{Tc}$ -pertechnetate scintigraphy cannot discriminate between Warthin's tumor and oncocytoma.

Because malignant transformation of Warthin's tumors is extremely rare, occurring in only 0.3% [15], a limited partial parotidectomy is the recommended treatment for Warthin's tumor. If reliable cytologic reporting is available, conservative management of Warthin's tumors is also considered appropriate for patients with significant comorbidities, making anesthesia high risk [16]. In contrast, because the recurrence rate of oncocytoma has been reported to be 20–30% in incomplete excision or multinodularity cases

[8], complete surgical excision is the treatment of choice for oncocytoma. In addition, oncocytic carcinomas are usually seen in association with a pre-existing oncocytoma [17]. Therefore, we emphasize the clinical significance of differential diagnosis between Warthin's tumor and oncocytoma.

Warthin's tumor is characterized by male predominance and lower pole location of parotid glands. However, an increase in the number of females over time and a decrease in the male–female ratio were observed [18]. One explanation for the decreasing male predominance may be the growing number of female smokers, because smoking is one of the main risk factors for developing Warthin's tumor [18, 19]. In addition, most Warthin's tumors involve



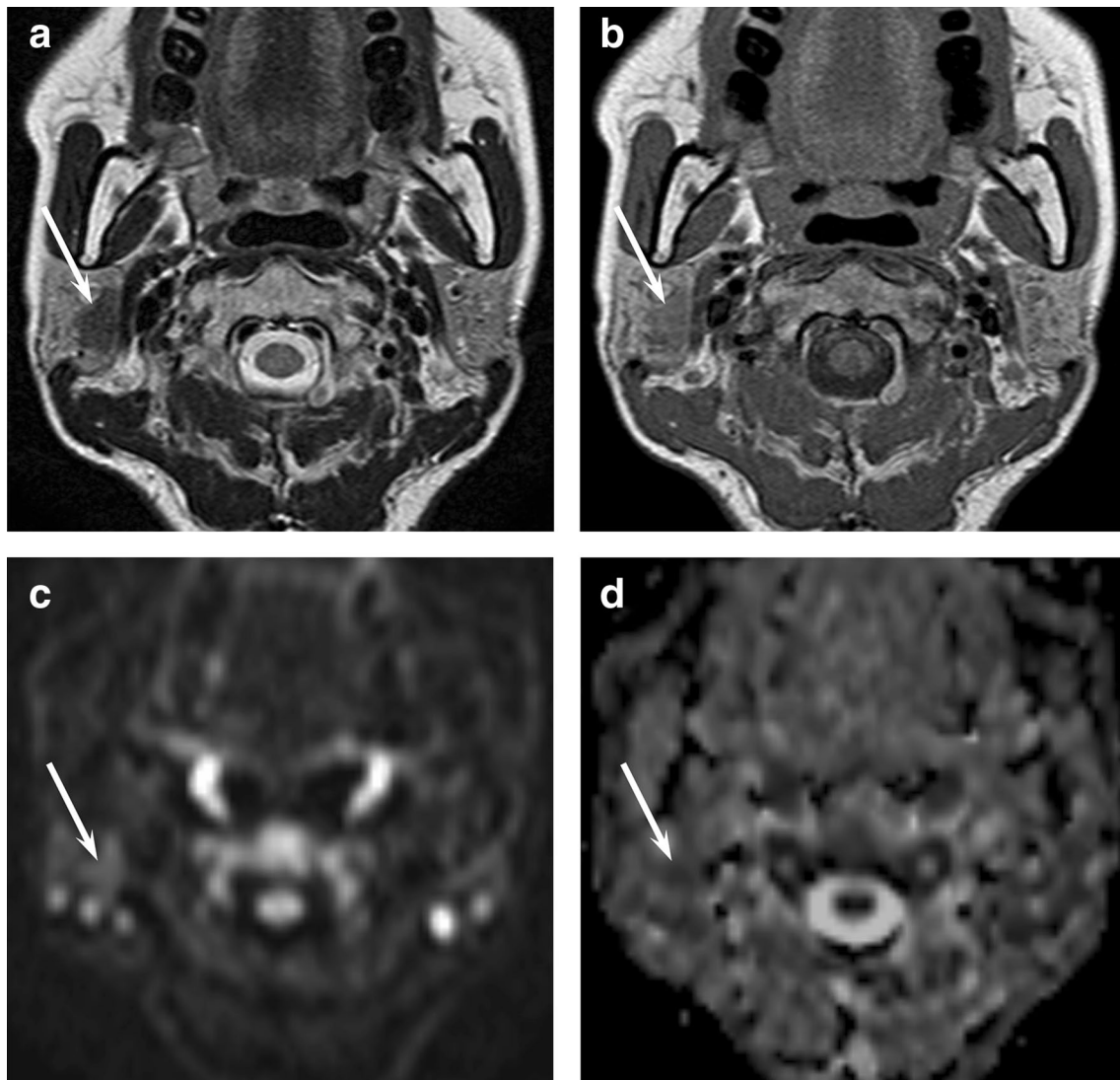


**Fig. 3** A 49-year-old woman with oncocytoma of the parotid gland. **a** T2-weighted MR image (TR/TE, 4102/90 ms) shows a homogeneously hypointense lesion (arrow) in the right parotid gland. **b** T1-weighted MR image (TR/TE, 827/9 ms) shows an isointense

lesion (arrow). **c** DW MR image (TR/TE/TI, 5,490/72/170 ms) shows a hypointense lesion (arrow). **d** ADC map shows intermediate ADC value ( $1.05 \times 10^{-3} \text{ mm}^2/\text{s}$ ) (arrow)

**Table 3** Qualitative imaging findings of Warthin’s tumor and oncocytoma

	Warthin’s tumor (n = 41)	Oncocytoma (n = 4)	p value
Lower pole location	36 (88)	1 (25)	0.014*
Multiplicity	10 (24)	0 (0)	0.351
Bilaterality	5 (12)	0 (0)	0.613
Intratumoral cysts	15 (37)	0 (0)	0.184

Data are numbers of patients, and numbers in parentheses are frequencies expressed as percentages

\* The frequency of Warthin’s tumors was significant higher than those of oncocytomas ( $p < 0.05$ )

the lower pole, but 10% are in the deep lobe. Therefore, because these clinical characteristics cannot always differentiate Warthin’s tumor from oncocytoma, the differential diagnosis by MR imaging is expected.

The solid components of Warthin’s tumor usually demonstrate iso- to hypointensity on T2-weighted images because it histopathologically consists of epithelial cells and lymphoid stroma with fibrovascular tissue. Most Warthin’s tumors vary from partly to predominantly cystic, and cystic formation has been reported in 30–60% of cases [4, 20]. Various numbers of cystic components filled with mucoid or brown fluid in Warthin’s tumor vary in size from small slit-like spaces to several centimeters in length and

occupy a considerable portion of the entire lesion. Focal hyperintense areas of Warthin's on T1-weighted images correspond to areas with accumulations of microscopic cysts, containing proteinous fluid with foamy cells, red cells, and neutrophils [5].

The solid components of oncocytoma usually demonstrate hypointensity on T2-weighted images, because it histologically consists of solid clusters or cords of tightly packed oncocytes separated by thin strands of fibrovascular stroma [7, 9]. Oncocytoma shows isointensity to the native parotid gland on both fat-suppressed T2-weighted images and fat-suppressed contrast-enhanced T1-weighted images [7].

Warthin's tumor might be indistinguishable from oncocytoma by traditional cross-sectional imaging alone [9]. Multiple or bilateral salivary gland tumors include Warthin's tumor, oncocytoma, basal cell adenoma, acinic cell carcinoma, adenoid cystic carcinoma, mucoepidermoid carcinoma, and other carcinomas [21]. Although cystic formation is a frequent imaging finding of Warthin's tumor [20], cystic components have been observed in 2 of 10 oncocytomas on contrast-enhanced CT [22]. In our study, although the SIRs on T2-weighted images were higher in Warthin's tumors than in oncocytomas, a considerable overlap was found between the two pathologies regarding the SIRs on T2-weighted images. Dynamic contrast-enhanced MR imaging can distinguish Warthin's tumor from other possible tumors except for oncocytoma [23]. Due to the hypervascular nature of Warthin's tumor, the high diagnostic accuracy of arterial spin labeling (ASL) allows the differentiation of Warthin's tumor from malignant tumor and pleomorphic adenoma [24]. However, oncocytomas also show a high signal intensity on ASL, suggestive of their hypervascular nature [9]. Some benign parotid tumors including pleomorphic adenoma, Warthin's tumor, and oncocytoma are known to be FDG avid, which decreases the specificity of PET/CT to differentiate malignant from benign parotid tumors [25–27].

DW imaging is useful to differentiate salivary gland tumors. However, ADCs alone did not allow the differentiation between benign and malignant salivary gland tumors because low ADCs for Warthin's tumor can overlap with those of malignant tumors. Low ADCs have been reported for Warthin's tumor due to the presence of epithelial and lymphoid stroma with microscopic slit-like cysts filled with proteinous fluid [5], and ranged from  $0.78$  to  $0.89 \times 10^{-3} \text{ mm}^2/\text{s}$  [6, 20, 28]. Meanwhile, ADCs for oncocytoma are reported to range from  $1.0$  to  $1.16 \times 10^{-3} \text{ mm}^2/\text{s}$  [8], and from  $0.8$  to  $1.0 \times 10^{-3} \text{ mm}^2/\text{s}$  [9]. However, we failed to find any reports comparing ADCs for Warthin's tumor and oncocytoma. In our study, the SIRs on DW images were higher in Warthin's tumors than in oncocytomas and ADCs were lower in Warthin's

tumors than in oncocytomas. In addition, little overlap was found between the two pathologies regarding the SIRs on DW images and ADCs. We assumed that the pathological characteristics of hypercellular lymphoid stroma with germinal centers in Warthin's tumor caused stronger diffusion restriction.

However, our study had some limitations. First, the study population was small, because this study was conducted at a single institution. Because oncocytoma is a rare salivary gland tumor, the number of oncocytoma cases was especially low. However, in spite of small number of oncocytoma cases, significant differences were found between Warthin's tumor and oncocytoma regarding the important MR findings for differential diagnosis. Second, we did not evaluate contrast-enhanced MR images, because contrast-enhanced MR imaging had only been performed in 1 of 4 patients with oncocytoma. Thus, we assessed the presence of cystic components on unenhanced MR images. Third, the visible solid components of Warthin's tumor have a broad range of MR signal intensity, because the extent of the signal intensity reflects the proportion of microcystic components and lymphoid stroma. Therefore, we might not be able to accurately evaluate solid components of Warthin's tumor on unenhanced MR images.

In conclusion, the localization of lower pole was more frequent in Warthin's tumors than in oncocytomas. The SIRs on T2-weighted images and those on DW images were higher in Warthin's tumors than in oncocytomas. ADCs were lower in Warthin's tumors than in oncocytomas. A considerable overlap was found between the two pathologies regarding the SIRs on T2-weighted images, whereas little overlap was found between the two pathologies regarding the SIRs on DW images and ADCs. If the accumulation of  $^{99\text{m}}\text{Tc}$ -pertechnetate is observed in the parotid gland tumors, DW imaging with ADC measurements would be useful for the differentiation of Warthin's tumor from oncocytoma of the parotid gland.

#### Compliance with ethical standards

**Conflict of interest** The authors declare that they have no conflict of interest.

#### References

1. Maiorano E, Lo Muzio L, Favia G, Piattelli A. Warthin's tumour: a study of 78 cases with emphasis on bilaterality, multifocality and association with other malignancies. *Oral Oncol.* 2002;38:35–40.
2. Miyake H, Matsumoto A, Hori Y, Takeoka H, Kiyosue H, Hori Y, et al. Warthin's tumor of parotid gland on Tc-99m pertechnetate scintigraphy with lemon juice stimulation: Tc-99m uptake, size, and pathologic correlation. *Eur Radiol.* 2001;11:2472–8.

3. Brandwein MS, Huvos AG. Oncocytic tumors of major salivary glands. A study of 68 cases with follow-up of 44 patients. *Am J Surg Pathol.* 1991;15:514–28.
4. Minami M, Tanioka H, Oyama K, Itai Y, Eguchi M, Yoshikawa K, et al. Warthin tumor of the parotid gland: MR-pathologic correlation. *Am J Neuroradiol.* 1993;14:209–14.
5. Ikeda M, Motoori K, Hanazawa T, Nagai Y, Yamamoto S, Ueda T, et al. Warthin tumor of the parotid gland: diagnostic value of MR imaging with histopathologic correlation. *Am J Neuroradiol.* 2004;25:1256–62.
6. Habermann CR, Arndt C, Graessner J, Diestel L, Petersen KU, Reitmeier F, et al. Diffusion-weighted echo-planar MR imaging of primary parotid gland tumors: is a prediction of different histologic subtypes possible? *Am J Neuroradiol.* 2009;30:591–6.
7. Patel ND, van Zante A, Eisele DW, Harnsberger HR, Glastonbury CM. Oncocytoma: the vanishing parotid mass. *Am J Neuroradiol.* 2011;32:1703–6.
8. Kasai T, Motoori K, Hanazawa T, Nagai Y, Ito H. MR imaging of multinodular bilateral oncocytoma of the parotid gland. *Eur J Radiol Extra.* 2007;63:97–100.
9. Iida E, Wiggins RH 3rd, Anzai Y. Bilateral parotid oncocytoma with spontaneous intratumoral hemorrhage: a rare hypervascular parotid tumor with ASL perfusion. *Clin Imaging.* 2016;40:357–60.
10. Liu RS, Yeh SH, Yen TC, Hsu DF. Salivary scintigraphy with vitamin C stimulation: an aid in differentiating unilateral parotitis from Warthin's tumor. *Eur J Nucl Med.* 1990;16:689–91.
11. Murata Y, Yamada I, Umehara I, Okada N, Shibuya H. Diagnostic accuracy of technetium-99m-pertechnetate scintigraphy with lemon juice stimulation to evaluate Warthin's tumor. *J Nucl Med.* 1998;39:43–6.
12. Sato T, Morita Y, Hamamoto S, Noikura T, Kawashima K, Matsune S, et al. Interpretation of scintigraphy of papillary cystadenoma lymphomatosum (Warthin's tumor) on the basis of histopathologic findings. *Oral Surg Oral Med Oral Pathol Oral Radiol Endod.* 1996;82:101–7.
13. Lusia S, Chodos RB, Lusia C, Chandramouly BS. Oxyphilic adenoma of the parotid gland. Identification with 99mTc-pertechnetate. *Radiology.* 1978;128:690.
14. Gates GA, Work WP. Radioisotope scanning of the salivary glands. A preliminary report. *Laryngoscope.* 1967;77:861–75.
15. Batsakis JG. Carcinoma ex papillary cystadenoma lymphomatosum. Malignant Warthin's tumor. *Ann Otol Rhinol Laryngol.* 1987;96:234–5.
16. Reddy VM, Thangarajah T, Castellanos-Arango F, Panarese A. Conservative management of Warthin tumour. *J Otolaryngol Head Neck Surg.* 2008;37:744–9.
17. Nakada M, Nishizaki K, Akagi H, Masuda Y, Yoshino T. Oncocytic carcinoma of the submandibular gland: a case report and literature review. *J Oral Pathol Med.* 1998;27:225–8.
18. Pinkston JA, Cole P. Cigarette smoking and Warthin's tumor. *Am J Epidemiol.* 1996;144:183–7.
19. Freedman LS, Oberman B, Sadetzki S. Using time-dependent covariate analysis to elucidate the relation of smoking history to Warthin's tumor risk. *Am J Epidemiol.* 2009;170:1178–85.
20. Kato H, Kanematsu M, Watanabe H, Mizuta K, Aoki M. Salivary gland tumors of the parotid gland: CT and MR imaging findings with emphasis on intratumoral cystic components. *Neuroradiology.* 2014;56:789–95.
21. Seifert G, Donath K. Multiple tumours of the salivary glands—terminology and nomenclature. *Eur J Cancer B Oral Oncol.* 1996;32B:3–7.
22. Tan TJ, Tan TY. CT features of parotid gland oncocytomas: a study of 10 cases and literature review. *Am J Neuroradiol.* 2010;31:1413–7.
23. Hisatomi M, Asaumi J, Konouchi H, Yanagi Y, Matsuzaki H, Kishi K. Assessment of dynamic MRI of Warthin's tumors arising as multiple lesions in the parotid glands. *Oral Oncol.* 2002;38:369–72.
24. Kato H, Kanematsu M, Watanabe H, Kajita K, Mizuta K, Aoki M, et al. Perfusion imaging of parotid gland tumours: usefulness of arterial spin labeling for differentiating Warthin's tumours. *Eur Radiol.* 2015;25:3247–54.
25. Shah VN, Branstetter B. Oncocytoma of the parotid gland: a potential false-positive finding on 18F-FDG PET. *Am J Roentgenol.* 2007;189:W212–4.
26. Seo YL, Yoon DY, Baek S, Lim KJ, Yun EJ, Cho YK, et al. Incidental focal FDG uptake in the parotid glands on PET/CT in patients with head and neck malignancy. *Eur Radiol.* 2015;25:171–7.
27. Kitajima K, Suenaga Y, Sugimura K. Present and future role of FDG-PET/CT imaging in the management of head and neck carcinoma. *Jpn J Radiol.* 2015;33:776–89.
28. Matsushima N, Maeda M, Takamura M, Takeda K. Apparent diffusion coefficients of benign and malignant salivary gland tumors. Comparison to histopathological findings. *J Neuroradiol.* 2007;34:183–9.